Am J Transl Res 2022;14(11):8103-8116
www.ajtr.org /ISSN:1943-8141/AJTR0143305

Original Article

Thoracic Jia-Ji electro-acupuncture mitigates low skeletal muscle atrophy and improves motor function recovery following thoracic spinal cord injury in rats

Xinyi Zhang[2,3,4*], Hailiang Xu[1,3*], Lei Zhu[1,3], Dageng Huang[1,3], Lingbo Kong[1,3], Zhiyuan Wang[1,3], Fang Tian[1,3], Botao Lu[1,3], Weidong Wu[1,3], Chao Jiang[1,3], Youjun Liu[1,3], Chengwen Wang[1,3], Shuaijun Jia[1,3], Yongliang Li[2], Minyi Yang[2], Xifang Liu[2], Dingjun Hao[1,3]

Departments of [1]Spine Surgery, [2]Rehabilitation, Xi'an Honghui Hospital, Xi'an Jiaotong University, Xi'an 710054, Shaanxi, China; [3]Shaanxi Key Laboratory of Spine Bionic Treatment, Xi'an 710054, Shaanxi, China; [4]The First Clinical Medical College of Shaanxi University of Chinese Medicine, Xianyang 712000, Shaanxi, China. [*]Equal contributors.

Received April 3, 2022; Accepted September 9, 2022; Epub November 15, 2022; Published November 30, 2022

Abstract: Objectives: The goal of this study was to determine whether electro-acupuncture (EA) stimulation might protect the motor endplate, minimize muscle atrophy in the hind limbs, and enhance functional recovery of rats with spinal cord injury (SCI). Methods: Sprague-Dawley adult female rats (n = 30) were randomly assigned into Sham, SCI, and EA + SCI groups (n = 10 each). Rats in the Sham and SCI groups were bound in prone position only for 30 min, and rats in the EA + SCI group were treated with electro-acupuncture. The EA was conducted from the first day after surgery, lasted for 30 mins, once every day for 28 consecutive days. Results: EA significantly prevented motor endplate degeneration, improved electrophysiological function, and ameliorated hindlimb muscle atrophy after SCI. Meanwhile, EA upregulated Tuj-1 expression, downregulated GFAP expression, and reduced glial scar formation. Additionally, after 4 weeks of EA treatment, the serum of SCI rats exhibited a reduced inflammatory response. Conclusion: These findings suggest that EA can preserve the motor endplate and reduce muscular atrophy. In addition, EA has been shown to improve the function of upper and lower neurons, reduce glial scar formation, suppress systemic inflammation, and improve axon regeneration.

Keywords: Electro-acupuncture, spinal cord injury, muscle atrophy, motor endplate, motor function recovery

Introduction

Spinal cord injury is a common disabling injury of the nervous system, which causes motor, sensory, urinary, and anal dysfunction and endangers the lives of patients [1]. According to a recent estimate, the annual incidence of spinal cord injury in the United States is approximately 54 cases per million people or approximately 17,000 new SCI cases per year [2]. SCI undergoes two stages: initial injury and secondary injury [3-5]. Primary spinal cord injury is often caused by compression, tear, distortion or shearing, which often results in axon fracture, nerve tissue destruction, and neuronal death. Then a cascade of intricate responses including edema, ischemia-reperfusion, inflammation, excitotoxicity, and oxidative stress-subsequently drives a secondary damage phase. Secondary damage from primary mechanical SCI can rapidly occur, resulting in an inflammatory response and neuronal death in the affected region [6, 7]. Long-term complications after SCI are quite common and severe, leading to reduced life expectancy and increased morbidity. This imposes a huge physical and emotional cost on individuals and families, and substantial financial burden on society. However, contemporary medicine currently lacks a viable pharmacological or methodological therapy for SCI. Therefore, the need for innovative treatment approaches for SCI has become critical.

With the advancement of medical equipment and technology in recent years, EA has become a hot spot for treating a variety of diseases. EA benefits from traditional acupuncture and el-

ectrical stimulation, and it can be rapidly performed following a standard stimulation protocol [8]. Studies have shown that EA is effective in lowering high blood pressure (BP) in clinical practice [9]. In addition, EA has been demonstrated to be effective in treating obesity [10] and is regarded as an effective and safe approach for treating stroke and diabetic peripheral neuropathy [11, 12]. Although EA has been proven to be an effective treatment for spinal cord injury, few studies have been conducted on muscle atrophy after spinal cord injury. Frequency is a crucial parameter of EA stimulation. The optimal frequency of electro-acupuncture differs a lot in different diseases, exhibiting frequency specificity [13]. Injury of upper and lower motoneurons can cause muscle atrophy. The integrity of the motor endplate plays an essential role in maintaining the morphology of the target muscle. However, the underlying mechanism responsible for the muscle atrophy after the effects of EA on spinal cord injury remains unclear.

Motor endplates are the connections between motor neuron axons and skeletal muscle fibers. The motor endplate connects alpha motor neurons in the anterior horn to skeletal muscle fibers [14]. The upper and lower motor neurons interact continuously under normal physiological circumstances. After a spinal cord injury, motor neurons cannot transmit nerve impulses to skeletal muscles, and rapidly denervated muscles atrophy. Studies have shown a 40%-60% reduction in skeletal muscle mass two weeks after spinal cord transection compared to the sham control group [15]. As a result, not only motor neurons in the spinal cord but also the neuromuscular junction (motor endplates) plays a role in healing,

As mentioned above, spinal cord injury leads to substantial alterations in muscles innervated below the level of damage. At present, many studies have been conducted to promote spinal cord repair with the aim of exploring the treatment effects of spinal cord injury. However, few studies investigating the degeneration and protective measures of muscle effectors at the distal end of the injured spinal cord and target organs have been conducted. Thus, this study aimed to determine whether EA stimulation to rats with spinal cord injuries might protect the motor endplate, minimize muscle atrophy in the hindlimbs, and enhance functional recovery.

Materials and methods

Animals

Thirty healthy, female Sprague-Dawley (SD) rats (eight weeks old, 200±20 g body weight) were purchased from the Laboratory Animal Center of Xi'an Jiaotong University (SVCM2021031-5019). All procedures were carried out in accordance with the Guidelines for Animal Care and Use (China) and approved by the Experimental Animal Ethics Committee of Shaanxi University of Chinese Medicine. In a controlled setting with a constant temperature of 20°C-25°C, 60±5% humidity, and a 12/12-h light/dark cycle, rats were fed normal fodder and readily available food and drink. Experiments were begun following a seven-day adaptation period. The animals were randomly divided into three groups: (1) Sham group, (2) SCI group (without treatment), and (3) EA + SCI group.

Spinal cord injury model

SCI models were created using procedures that have been previously published [16]. All rats were sedated intraperitoneally with 1% pentobarbital sodium (50 mg/kg). To completely expose the spinal cord, the T10 vertebral lamina and spinous process were removed using rongeur forceps, and a substantial crush damage was produced for 60 sec with a vascular clip (30 g forces, Oscar, Shanghai, China). The Sham group of rats received the same surgical treatment as the other rats, but were not compressed. The rats were then placed on heating pads until they recovered from anesthesia and were able to return to their clean cages. To avoid infection, the rats' bladders were manually expressed three times daily after surgery, and all animals were given an intramuscular injection of penicillin (160,000 U/ml/d).

Electro-acupuncture stimulation

For EA treatment, the rats were immobilized in wooden holders. Rats were given EA therapy at the T9 and T10 Jiaji (EX-B2) acupoints, which were placed on opposite sides of the dorsal section of the spine, proximal and distal to the damaged segment 16 (**Figure 1A**) [17]. We used sterilized disposable stainless steel needles (0.25 mm × 25 mm diameter). The needle

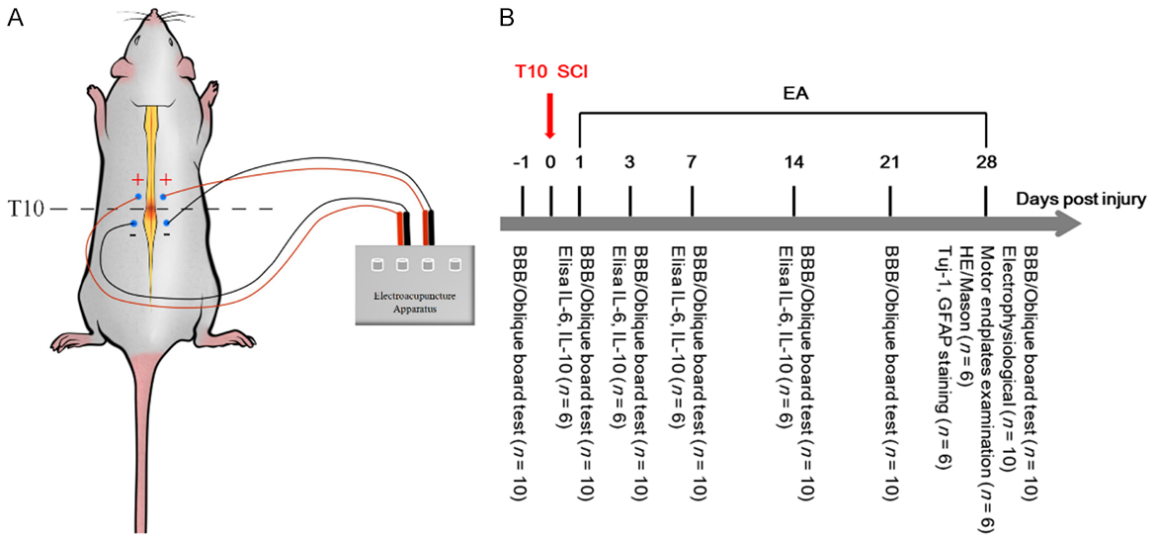

Figure 1. Schematic diagram of EA and experimental procedure. A. A schematic diagram illustrates the location of selected Jia-Ji acupoints in a rat, and shows the method of the electrical stimulation conducted by electroacupuncture apparatus. B. Experimental protocol: all rats were fed adaptively for 7 days and randomly divided into three groups: Sham group (n = 10), SCI group (n = 10) and EA + SCI group (n = 10). Spinal cord injury models were made in SCI group and EA + SCI group. The EA + SCI group started intervention from the first day postsurgery. The rats in the Sham group and SCI group were bound with 30 min with a rat retainer during electro-acupuncture. Finally, Corresponding indexes were detected at each time point.

was pushed 4-5 mm into the skin until it hit the erector spine, and then it was attached to a pair of electrodes from the acupuncture nerve stimulator. The parameters were set as follows: a square wave output at 20 Hz and a current intensity of 1 mA, which caused mild vibration of the muscles around the acupuncture sites. The EA was conducted from the first day after the surgery and lasted 30 min, once every day for 28 consecutive days. Rats in the Sham and SCI groups were bound in prone position only for 30 min, and rats in the EA + SCI group were treated with electro-acupuncture. Experimental protocols are illustrated in **Figure 1B**.

Hindlimb exercise score

The Basso, Beattie, and Bresnahan (BBB) score, which has 22 grades ranging from 0 to 21, is used to evaluate the recovery of hind limb motor function in rats after SCI [18]. Complete paralysis is indicated by a score of 0, whereas full motor function is indicated by a score of 21. The rats' bladders were manually expressed before the test to reduce the impact of a full bladder on locomotor activity. Three minutes were spent watching rats in an open field. Each rat was measured three times, and the average integer value was recorded. Two assessors blinded to the experimental groups collected and analyzed BBB scores 1 day before surgery and 1, 3, 7, 14, 21, and 28 days after damage.

Oblique board test

The oblique board test was performed on pre-injury day 1 as well as post-injury days 1, 3, 7, 14, and 28. The rats were placed on a board with one side attached to the ground and the board gently lifted to fix the opposite side. The rats' greatest angle was measured when they remained on the board for 5 sec without falling. After each rat was examined three times, the average value was used to determine the final conclusion.

Electrophysiological recording

Electrophysiological recordings were carried out as previously described 4 weeks after SCI. Electrophysiological studies were done on the hind limbs after subcutaneous anesthesia with 1% pentobarbital sodium (50 mg/kg). The anesthetized rat was fixed in a stereotaxic apparatus (model 1404, David Kopf, Tujunga, CA, USA), and the scalp was exposed. The gastrocnemius muscle in the hindlimbs was used to elicit Motor Evoked Potentials (MEPs). The stimulus strength (approximately 1.0-3.0 mA) and stimulus frequency (0.2 ms and 1.9 Hz,

respectively) were adjusted to a reasonable range. The recording electrode was inserted in the relevant cortical sensory area for SEP signals (beneath the scalp near the coronal and sagittal sutures). The recording electrode was positioned 0.5 cm behind the reference electrode. In addition, rats' tails were immersed in saline solution when MEPs and Somatosensory Evoked Potential (SEPs) were measured. The latency and amplitude of MEP and SEP were analyzed.

Motor endplates examination

To identify the motor endplate distribution and morphology, the gastrocnemius muscles of rats were stained with the Acetylcholinesterase (AChT) Staining Solution Kit (cupric ferrocyanidetechnique)(Solaibio,Beijing,China).Themuscles were embedded in the Tissue-Tek O.C.T. compound, and serial 7 μm slices were cut and mounted onto polylysine-coated slides using a Frozen Slicer (Leica CM1950, Germany).

Gastrocnemius muscle wet weight

After meticulous dissection of accompanying tendons and fascia, the gastrocnemius of both lower limbs were completely removed. Then, the rats in each group were weighed with a precision weighing scale (0.01 g) on absorbent filter paper, and the average wet weight of the gastrocnemius of each group was compared.

Hematoxylin-eosin and masson staining

All animals were sacrificed by intraperitoneal injection of an overdose of sodium pentobarbital at the experimental endpoint, and their gastrocnemius muscle and myocardium were detected. The mid-belly of the gastrocnemius muscle and the left ventricular myocardium were fixed, dehydrated, embedded in paraffin, and sectioned transversely with a paraffin microtome at a thickness of 5 mm (Leica RM 2235, Germany). One section of every 100 m of the chosen muscle segment was stained with hematoxylin and eosin (HE), for a total of three sections per rat. Images of five random fields of each muscle segment were captured using a bright field microscope (Leica DM IRB) at a standard magnification of 10 x. The section area (CSA) of gastrocnemius muscle fibers was quantified using Image J software (NIH, USA). To assess the impact of electroacupuncture on the myocardium, we evaluated the degree of myocardial fibrosis in the left ventricle. According to the manufacturer's protocols, the left ventricular myocardium was stained with hematoxylin-eosin or Masson (Solaibio, Beijing, China). Five random fields were selected from the three sections obtained from each animal for observation under a brightfield microscope (Leica DM IRB) image analyzer. Hematoxylin-Eosin and Masson staining methods were as described previously [19, 20].

Immunofluorescence staining of Tuj-1 and GFAP

The animals were perfused transversally with 100 mL cold physiological saline and 300 mL 4% paraformaldehyde-phosphate buffer solution after 4 weeks. After being stored in 4% paraformaldehyde overnight, the spinal cords were extracted and cryoprotected in 0.1 M phosphate buffer containing 30% sucrose at 4°C. On a frozen microtome, the spinal cord was cut longitudinally, and 8 sets of every 5th serial section were mounted on gelatin-coated glass slides. The immunofluorescence staining was done as described previously [21]. All samples were blocked in PBS supplemented with 0.3% Triton X-100 and 10% normal donkey serum for 1 h. The primary antibodies were incubated at 4°C overnight. Samples were treated with secondary antibodies (1:200, Abcam) and DAPI (1:1000, Abcam) after washing in PBS, and fluorescence microscopy was used to examine them. The primary antibodies were anti-Tuj-1 (neuronal marker, 1:300, Abcam) and anti-GFAP (astrocyte marker, 1:300, Abcam).

Measurement of IL-6 and IL-10 levels in serum

Whole blood samples were collected from the rats' tails in each group at 1, 3, 7, and 14 days post-injury (dpi). The samples were centrifuged for 10 min at 3000 rpm and separated to obtain serum after 10-20 min of spontaneous coagulation at room temperature. Then, the levels of IL-6 and IL-10 in rat serum were quantified using commercial ELISA kits (Jiangsu Enzyme Industrial Co., Ltd, China), according to the manufacturer's instructions. According to the manufacturer's specifications, the absorbance was measured at 450 nm. The IL-6 and IL-10 content of each sample was evaluated using the standard curve, and the IL-6 and IL-10 levels were expressed in pg/mg protein.

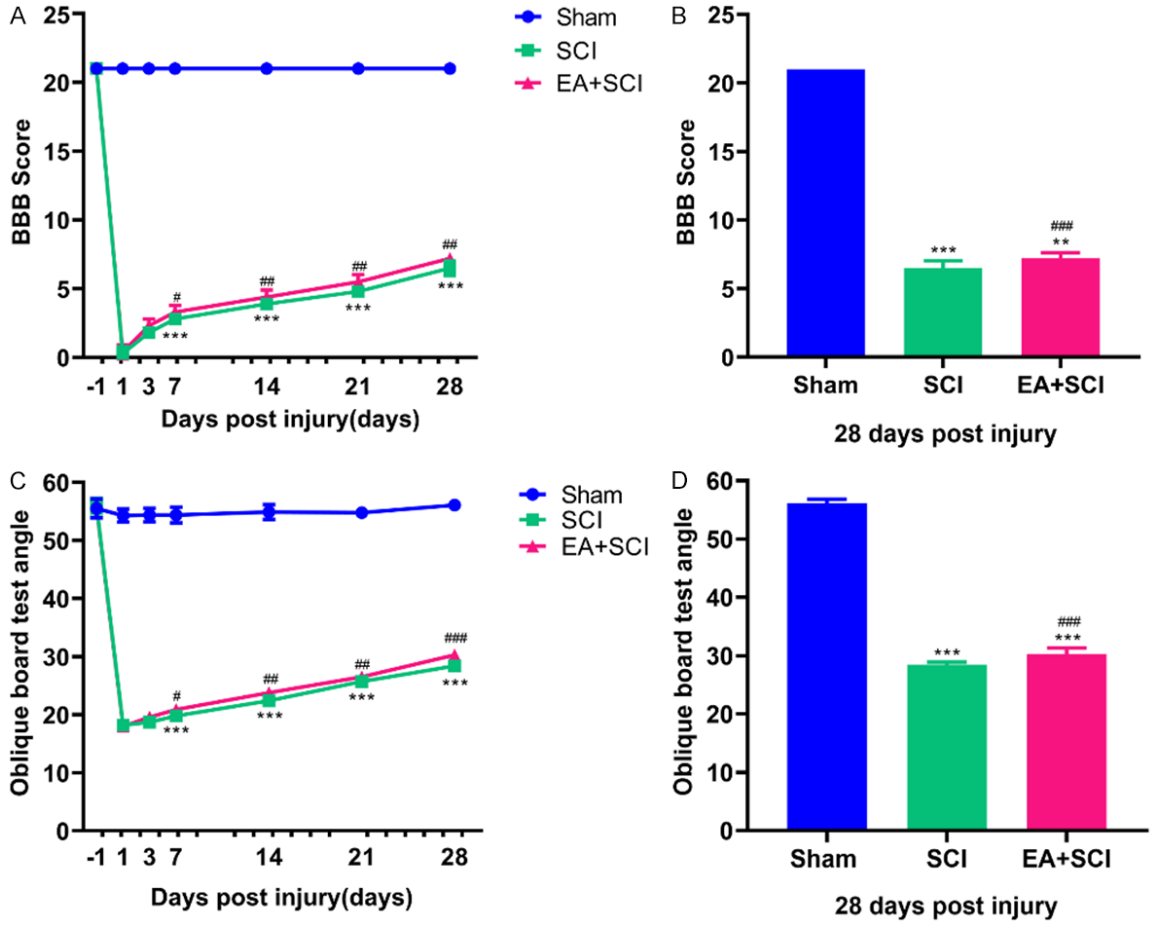

Figure 2. EA improved locomotor functional recovery after SCI. A, C. Locomotor function in the hindlimbs was evaluated by BBB score and oblique board test at -1, 3, 7, 14, 21, and 28 days post injury. B. Quantification of the BBB score on day 28 in each group. D. Quantification of the oblique board test angle on day 28 in each group. $^{*}P < 0.05$, $^{**}P < 0.01$, $^{***}P < 0.001$ compared with Sham group; $^{\#\#\#}P < 0.001$ compared with SCI group. ($n = 10$).

Statistical analysis

The statistical significance of the difference between groups was determined using a one-way analysis of variance, followed by the post-doc least significant difference range test. Data are expressed using the mean and standard deviation (SD) of at least three separate experiments. A statistically significant difference was identified as one with a $P < 0.05$. SPSS version 25 was used for the analysis.

Results

EA improved hindlimb motor function after SCI in rats

Normal rats had a baseline BBB score of 21 points. After the SCI model was established, rats in the sham-operated group showed normal function with a BBB score of 21. SCI reduced locomotor performance as measured by the BBB rating scale. Over the 4 weeks, a gradual recovery was observed in all SCI groups. The EA + SCI group showed lower BBB scores than the sham group at 7, 14, 21, and 28 days ($P < 0.001$). On these time points, the BBB scores in the EA + SCI group were somewhat higher than those in the SCI group ($P < 0.05$) (**Figure 2A**, **2B**). At 7, 14, 21, and 28 days after the oblique board test, the EA + SCI group had a smaller angle than the sham group ($P < 0.001$). In comparison to the SCI group, the angle was slightly larger in the EA + SCI group at these time points ($P < 0.05$) (**Figure 2C**, **2D**). These results showed that EA improved hind limb motor function at 7, 14, 21, and 28 days after spinal cord injury.

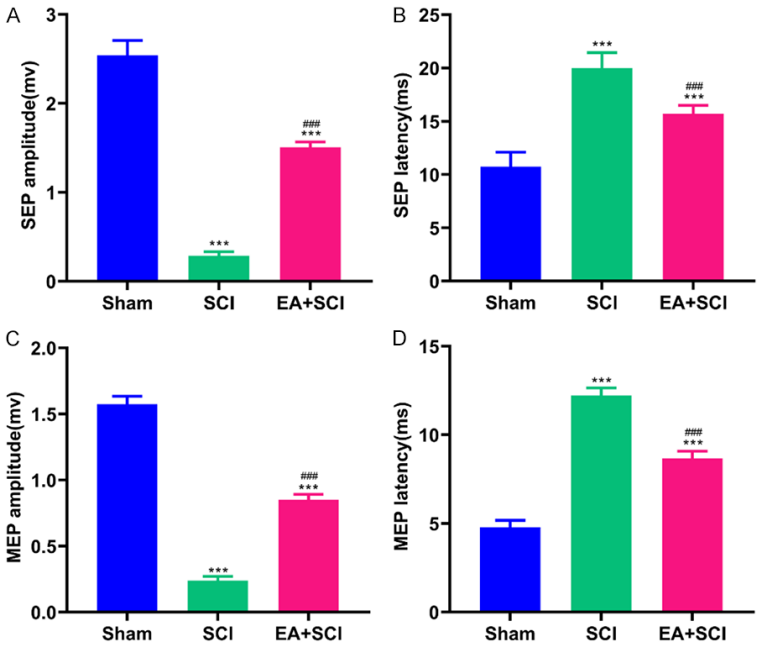

Figure 3. EA contributed to electrophysiological recovery after SCI. The plots showed the amplitude (A) and latency (B) of SEPs. The plots showed the amplitude (C) and latency (D) of MEPs. ***P < 0.001 compared with Sham group; ###P < 0.001 compared with SCI group. Data are represented as mean ± SD, (n = 10).

EA contributed to electrophysical recovery after SCI

The latency and amplitude of SEPs and MEPs suggested the recovery of electrophysiological function. The amplitude and latency of the MEP and SEP are commonly assumed to indicate the number of excited axons and the nerve's conduction velocity, respectively, as extensively used clinical evaluation criteria. As seen in **Figure 3A** and **3B**, SCI increased the average signal to response latency (19.970±1.462 ms, compared to 10.730±1.383 ms in the Sham group, P < 0.001) and decreased the mean amplitude of SEPs (0.288±0.045 mv, compared to 2.540±0.167 mv in Sham group, P < 0.001). EA shortened the latency (15.710±0.790 ms, compared to 19.970±1.462 ms in SCI group, P < 0.001) and raised the amplitude (1.505±0.063 mv, compared to 0.288±0.045 mv in SCI group, P < 0.001) of SEPs. **Figure 3C** and **3D** illustrate the MEP amplitude and latency of the Sham, SCI, and EA + SCI groups 28 days after SCI. The results showed that the latency of MEP in the SCI group (12.220±0.434 ms) was longer compared with the Sham group (4.787± 0.389 ms; P < 0.001), but EA inhibited the increase in latency (EA + SCI group: 8.668±0.413 ms). The EA + SCI group generated a higher amplitude than the SCI group (EA + SCI group vs. SCI group: 0.850±0.041 mv vs. 0.239±0.032 mv, P < 0.001). These data indicated that EA aided in recovering electrophysiological function following SCI.

EA protected the function and morphology of the motor endplate

As shown in **Figure 4**, the blue nucleus can be observed under light microscopy following AChT labeling. The motor endplate longitudinal aggregation distribution site on the muscle fibers appears dark brown. MEP was less dispersed and the waveform shape changed in the gastrocnemius muscle of rats after spinal cord injury compared to the sham group. The number of motor endplates in the EA + SCI group was more than that in the SCI group. This finding could indicate that the motor endplate of the gastrocnemius of SCI rats underwent pathological alterations in structure. To some extent, EA can protect the motor endplate of rats following spinal cord injury.

EA mitigated low skeletal muscle atrophy and increased the gastrocnemius muscle wet weight

The gastrocnemius muscle's wet weight and cross-sectional area of muscle fibers were measured 28 days after spinal cord injury (**Figure 5**). Substantial skeletal muscle atrophy could result from a spinal cord injury. The degree of gastrocnemius muscle loss was determined among the three groups of rats. The SCI group showed significantly lower wet weight than the EA + SCI group at 4 weeks after the injury 18.1% (P < 0.001). Hematoxylin-eosin-stained transversely sectioned gastrocnemius muscle further showed that SCI caused gastrocnemius muscle fiber atrophy in both SCI groups. Initially, the cross-sectional areas of the SCI groups decreased. We can calculate muscle fiber diameter according to

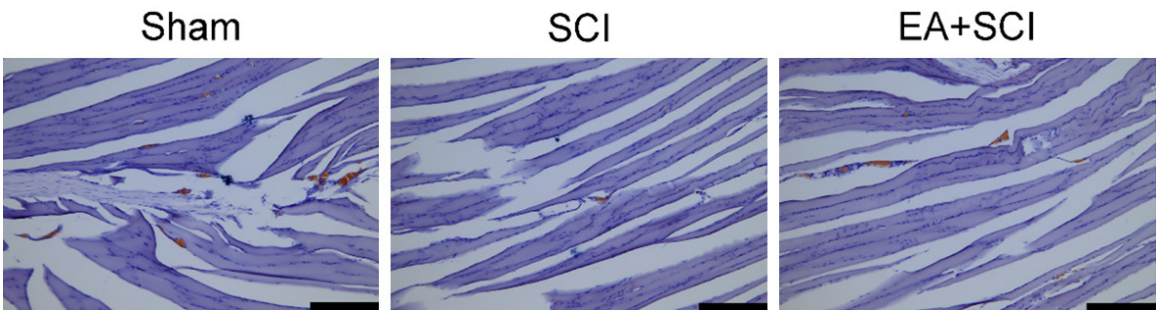

Figure 4. Evaluation for improving effects of EA on motor endplate activity by testing the acetylcholinesterase levels. Images for acetylcholinesterase stained gastrocnemius tissues. The site of the motor endplate appears as a dark brown color after the AChE staining. The nucleus is blue. Scale bars = 200 μm. *n* = 6 rat per group.

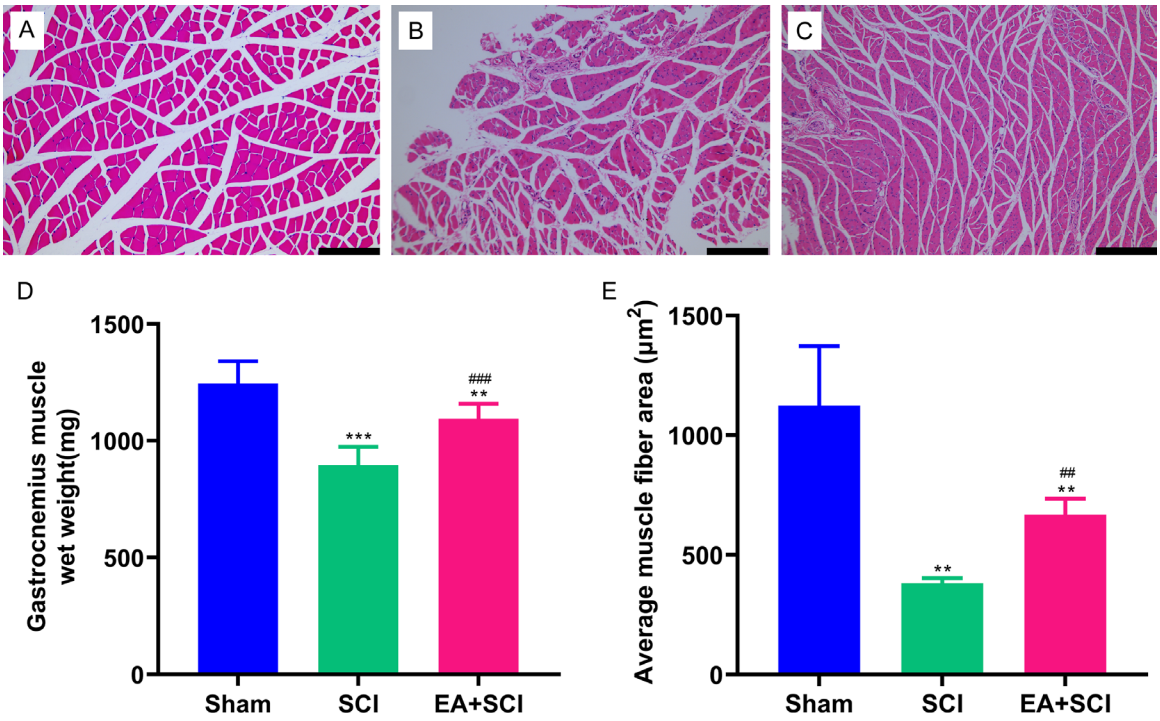

Figure 5. EA treatment alleviated skeletal muscle atrophy following spinal cord injury. (A-C) Representative muscle fibers stained by hematoxylin and eosin are displayed in the Sham, SCI, and EA + SCI groups, respectively. (D) Wet weight of gastrocnemius muscle. (E) Quantification of cross-sectional area (μm^2) of gastrocnemius muscle fibers. $^{**}P < 0.01$, as compared with the Sham group; $^{\#\#}P < 0.01$, as compared with the SCI group. Data are presented as mean ± SD. *n* = 6, Scale bars = 200 μm in (A-C).

the cross-sectional area of the muscle fiber, which reflects muscular atrophy more directly. At 4 weeks, the mean area of the SCI group was significantly lower than that of the EA + SCI group at 42.8% ($P < 0.01$). Additionally, it was discovered that EA therapy could partially reduce muscle fiber atrophy. Compared to the Sham group, the muscle conditions of the EA-treated rat did not fully recover to the projected level ($P < 0.05$). Thus, EA can alleviate muscle atrophy in rats following spinal cord injury to a certain extent.

EA attenuates neurologic damage and promotes neuroregeneration after SCI

To elucidate the effects of EA on the protection of nerve, immunofluorescence staining was used to quantify Tuj-1 and GFAP. **Figure 6A** shows that the GFAP-positive glial scar and Tuj-1-

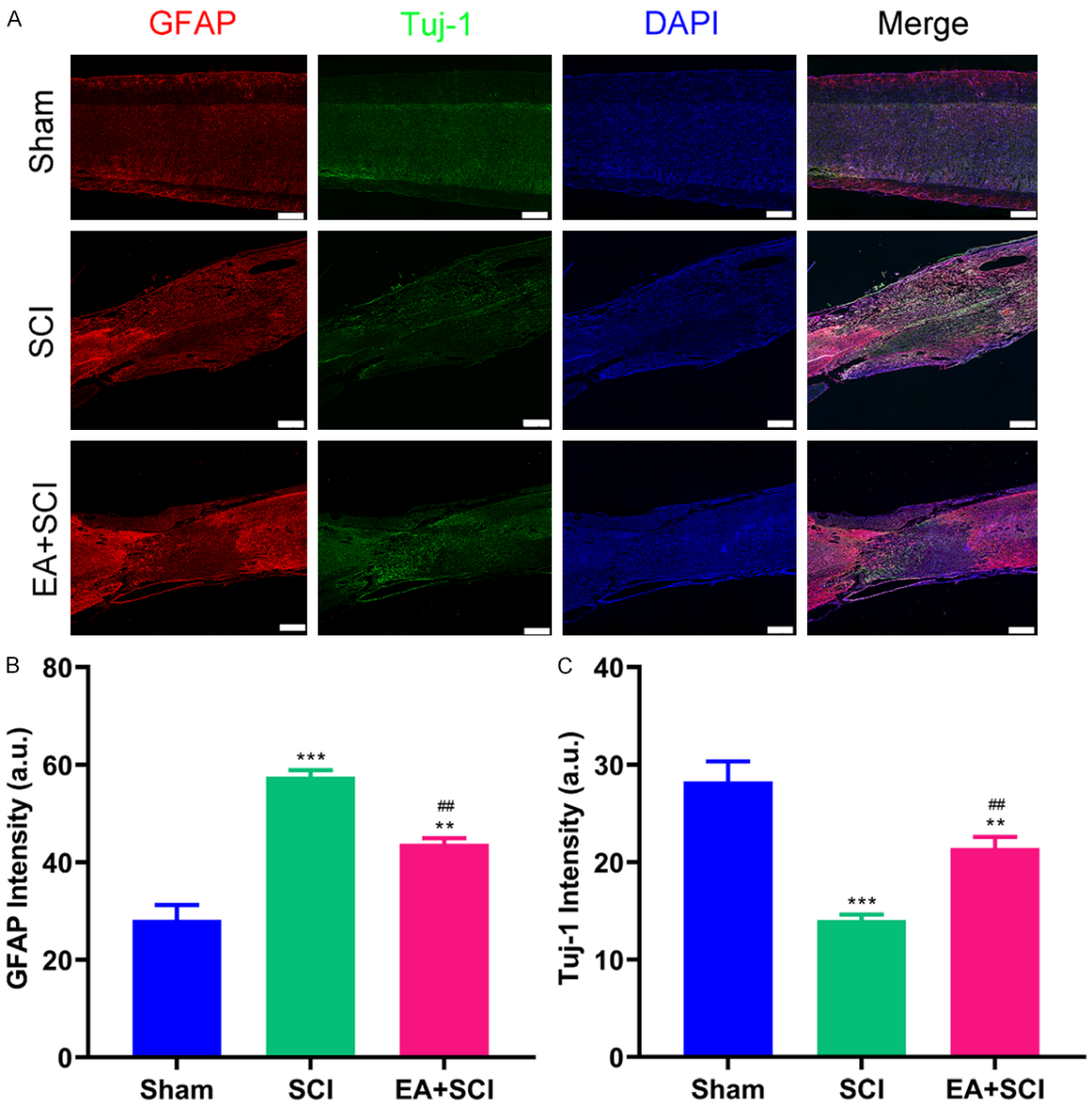

Figure 6. Immunofluorescence staining of spinal cord tissue and evaluation. (A) Immunofluorescence of SCI staining with astrocytes marker GFAP and neuron marker Tuj-1. Intensity analysis of (B) astrocytes marker GFAP expression, (C) neuron marker Tuj-1 expression. $^{**}P < 0.01$, $^{***}P < 0.001$ as compared with the Sham group; $^{\#\#}P < 0.01$, as compared with the SCI group. Data are presented as mean ± SD. $n = 6$, Scale bars = 400 μm.

positive cells were present at the lesion site 4 weeks after SCI. As demonstrated in **Figure 6B**, EA therapy substantially suppressed the astrocytic response and decreased the severity of early gliosis following SCI in the EA + SCI groups. The intensity of GFAP in the SCI group was higher than that in the EA + SCI group (SCI group compared with the EA + SCI group: 57.550± 1.348 vs. 43.760±1.171). In addition, compared to the SCI group (**Figure 6C**), more Tuj-1 appeared in the lesion area of the EA + SCI group (21.450±1.132), suggesting that EA facilitated the differentiation of neural stem cells into neurons. The result indicates that neurons degenerated in the lesion site of the SCI group in the absence of therapy.

Effect of EA on the levels of IL-6 and IL-10 in the serum of rats

Inflammation has a role in SCI pathophysiology, and severe inflammation destroys normal tissue and slows functional recovery. The release of inflammatory cytokines that promote

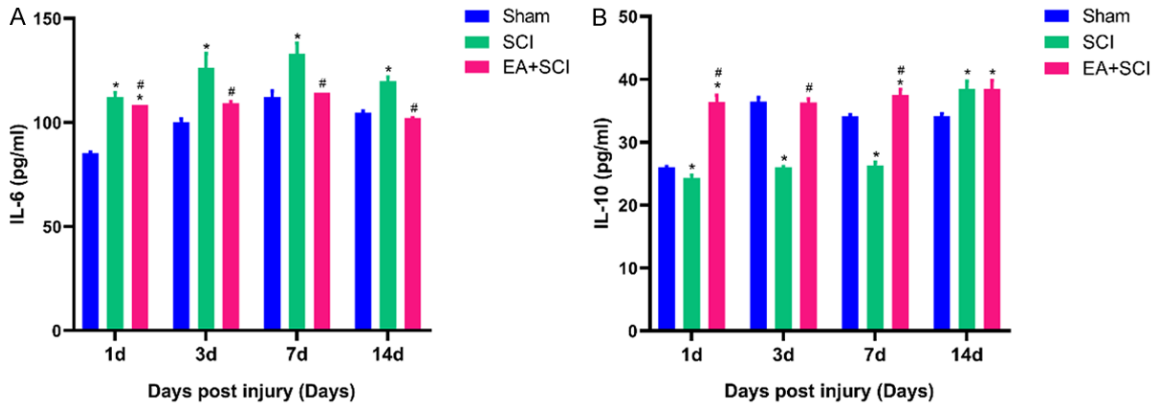

Figure 7. Effect of EA on serum inflammatory cytokine concentrations in SCI rats. Serum concentrations of IL-6 (A) and IL-10 (B) inflammatory cytokines were detected by ELISA. Standard curves were constructed by plotting the mean absorbance for each standard on the X -axis against the concentration on the Y-axis and a best fit line was drawn, determined by regression analysis. *$P < 0.05$, as compared with the Sham group. #$P < 0.05$, as compared with the SCI group. Data are expressed as the mean ± SD ($n = 6$; one-way analysis of variance and Tukey's post hoc test). The experiment was repeated in triplicate.

cell death and tissue degradation characterizes early microglia/macrophage recruitment following SCI. On days 1, 3, 7, and 14 following the surgery, ELISA was used to examine the expression of the pro-inflammatory cytokine IL-6 and the anti-inflammatory cytokine IL-10 in the serum of each group. As shown in **Figure 7**, IL-6 levels were significantly upregulated at 1, 3, 7, and 14 days after SCI in the SCI group compared to that in the Sham and EA + SCI groups ($P < 0.05$), reaching a peak at 7 days. The corresponding IL-6 levels in SCI group were 112.292±2.165, 126.333±6.813, 132.986±5.172, and 119.792±2.165 pg/ml at 1, 3, 7, and 14 days post-SCI, respectively. IL-10 levels were substantially upregulated at 1, 3, and 7 days after SCI in the EA + SCI group compared to that in the SCI group ($P < 0.05$). The corresponding IL-10 levels in the EA + SCI group were 36.402±1.096, 36.332±0.566, 37.509±0.932 pg/ml at 1, 3, and 7 days post-SCI, respectively. The IL-10 level in serum was significantly increased in the SCI group at 14 days after SCI (38.472±1.266 pg/ml). However, there was no significant difference compared to the EA + SCI group at 14 days after SCI.

Effect of EA on the myocardial fibrosis of rats after SCI

The myocardial tissue was taken for HE and Masson staining to observe the changes in the myocardium. As shown in **Figure 8**, there was no significant difference among the three groups. HE showed that there was no significant difference in the infiltration of inflammatory cells and cardiomyocytes in rats. The fibrotic response is crucial for maintaining the structure of the heart and sustaining cardiac function in response to injury. The collagen fiber network linking neighboring cells was intact, and the collagen fiber quantity was reduced, indicating that the collagen distribution (Masson positive material) was virtually uniform.

Discussion

The present study investigated whether EA can alleviate skeletal muscle atrophy after SCI. We have confirmed that EA at Jiaji points could protect motor endplate and prevent hindlimb muscle atrophy following SCI. Moreover, EA enhances the recovery of locomotor functions, facilitates the electrophysiological recovery after SCI, elevates the expression levels of Tuj-1, and inhibits the expression levels of GFAP at biologically plausible time points after SCI. At the same time, EA is safe to a certain extent by inhibiting inflammation in the serum of SCI rats and has no adverse effects on the myocardium. Such injury-induced secondary effects on linked musculature that are not directly related to the damage may give new therapeutic targets for improving functional recovery after SCI.

EA is a traditional Chinese medicine therapy that is often utilized in clinical settings to enhance the prognosis of spinal cord and neuro-

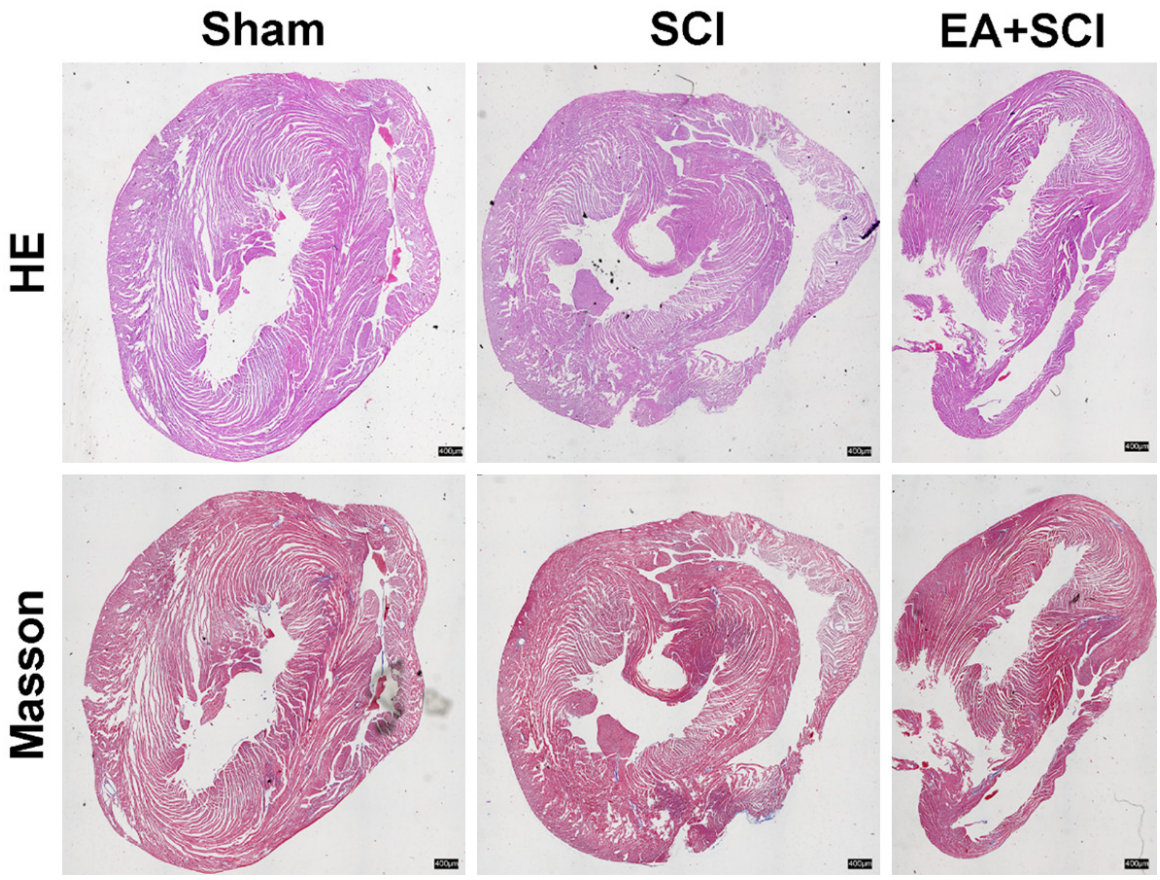

Figure 8. Effect of EA on the myocardial fibrosis of rats after SCI. Representative photomicrographs of HE and Masson's staining of the myocardium of rats. *n* = 6, Scale bars = 400 μm.

muscular injuries. After SCI, EA at Jiaji sites combines acupuncture and electric field effects on the damaged spinal cord. The Huatuo Jiaji points are 34 acupoints located 0.5 inches lateral to the first thoracic and fifth lumbar vertebras in the human body. Based on anatomy, EA on Jiaji points can stimulate the appropriate posterior ramus of the spinal nerve originating from the lower vertebrae. Numerous clinical investigations have established that EA has a definite effect on spinal cord injury [22]. Scholars have also conducted much research on the mechanism of electro-acupuncture, which is shown in the following aspects: Electro-acupuncture has been shown to inhibit the inflammatory response and oxidative stress [23-26], reduce ischemia and hypoxia [27], inhibit cell death [28], reduce glial scar formation [29], and secrete a variety of nerve growth active substances to promote nerve cell growth, axon regeneration and remyelination [30-32]. After spinal cord injury, severe muscular atrophy develops in lower limb muscles due to long-term denervation and disuse. There is evidence that EA has a favorable effect on muscular atrophy therapy [33, 34]. According to the current findings, EA is beneficial to the survival of motor endplates in SCI and improves the atrophy of muscles afflicted by the spinal cord damage. On the other hand, the BBB test is a valuable approach for assessing free locomotive behavior in animals with spinal cord injuries. In our study, the BBB score was higher in the EA + SCI group after 7 days at various time points than the SCI group, demonstrating that EA contributes to the recovery of hind limb motor function. These findings serve as an important experimental benchmark for EA in the treatment of SCI.

Disuse atrophy is caused by the loss of higher motor neurons, which occurs in SCI or lower motor neurons (denervation) [35]. Recovery of motor function after a spinal cord injury is dependent on the nervous system's ability to

self-repair and the integrity of the motor endplate [36, 37]. However, the speed of self-repair of the nervous system is slow. Once the target muscle begins to atrophy, the motor endplate loses its integrity and becomes challenging to control again. The spinal cord motor nerve has a nutritional effect on the target muscle [38, 39]. Neurotrophic factors are found in the motor neurons of the spinal cord, which help to preserve the morphology of the target muscle and the normal function of the motor endplate. As shown in **Figure 4**, the number of motor endplates in the EA + SCI group was more than that in the SCI group. This suggests that EA can protect the motor endplate. Sciatic nerves dominate the hindlimbs. Anatomically, 60%-70% of the spinal fibers that comprise the sciatic nerve originate from the L5 segment [40]. EA on Jiaji points can excite the same posterior ramus of the spinal nerve that originates from the lower vertebrae, as expected. The EA + SCI group had a higher BBB score, wet weight, and gastrocnemius muscle fiber cross-sectional area than the SCI group in the hindlimbs. As a result, our findings showed that EA is essential for sensory afferent projections to spinal motor neurons, and has the ability to change their connections. EA in thoracic Jiaji points shows the superior protective effects of lower motor neurons.

We must also consider on the safety aspects and side effects of EA. The frequency and wave type of EA are critical for individuals undergoing SCI functional rehabilitation. Based on electrophysiology, the optimum electric current and frequency should be determined. Previous research has shown that EA stimulation at 50 Hz improves motor function continuously and significantly, whereas EA stimulation at 100 Hz improves locomotor activity noticeably but not significantly [41]. By improving lysosomal function, boosting autophagy flux, lowering necroptosis, and regulating neuron death, Yin et al. demonstrated that EA stimulation at 100 Hz can recover hind limb motor function in rats following SCI [17]. By blocking the Notch signaling pathway via manipulation of the H19/EZH2 axis, Geng et al. discovered that electrical stimulation at a frequency of 2 Hz can speed SCI rats' recovery and promote the proliferation and differentiation of neural stem cells (NSCs) [42]. Our study found that EA stimulation at 20 Hz preserved the motor endplate and reduced muscle atrophy of the hindlimbs after SCI. EA stimulation (60 Hz for 1.05 s and 2 Hz for 2.85 s, pulse width 0.5 ms) was discovered by Zhang et al. to help with muscle atrophy in the hindlimb [34]. It also enhances the expression of NT-3 and ChAT, which is specifically located in the ventral horns of lumbar motor neurons. This suggests that different waveform electric acupunctures have a similar effect. Pro-inflammatory cytokines, such as IL-1, IL-6, and IL-10, are critical contributors in secondary injury. Our studies found that EA decreased inflammatory factors (IL-6 and IL-10), suggesting that EA suppressed the inflammatory reaction. Furthermore, the Masson staining results showed that the fibrosis area in the SCI group and EA + SCI group had no significant difference compared with the sham group. This indicates that electro-acupuncture causes no damage to the myocardium and is safe to some extent. Overall, our results collectively suggest that EA stimulation allows a wide range of parameters and can inhibit inflammation, and shows certain level of safety.

Tuj-1 is a β-III tubulin that is thought to be involved in the cell type-specific differentiation of neurons. Antibodies to Tuj-1 are often used to mark the early stages of neuronal differentiation [43]. When the synaptic differentiation of neurons is impaired, the expression level of Tuj-1 is decreased, and Tuj-1 can be used as a specific marker of synaptic differentiation [44]. Glial fibrillary acidic protein (GFAP) is one of the greatest predictors of astrocyte activation in the central nervous system after injury or stress [45]. After spinal cord injury, astrocytes were activated, underwent structural and functional changes, and the expression level of the structural protein GFAP was significantly increased [46, 47]. The early glial scar can protect the damaged area and improve the microenvironment, but the glial scar is a physical and chemical barrier. The role of glial scar in inflammation and axonal regeneration has long been regarded as a double-edged sword. Astrocytes respond to central nervous system injury by proliferation and glial scar formation [48]. Therefore, immunofluorescence was used to examine these two types of proteins, and the results are displayed in **Figure 6**. The expression of tuj-1 in the SCI group was lower than that in the other two groups. In comparison to Tuj-1, an opposite tendency may be observed

for GAFP expression. The SCI group expressed more GFAP than the EA + SCI group. This suggests that early intervention by EA after spinal cord injury can downregulate GFAP expression and reduce astrocyte activation, decreasing the development of glial scars. As indicated previously, EA has been proven to successfully promote spinal cord repair by favoring the creation of new neurons and suppressing astrocyte growth. Collectively, our findings shed light on the mechanisms behind the efficacy of electro-therapeutic acupuncture in the treatment of SCI.

In conclusion, the results showed that EA at EX-B2 could protect the motor endplate, reduce muscle atrophy of the hindlimbs, and recover the motor function after SCI. In addition, EA can protect neurons, reduce glial scar formation, and improve axon regeneration. Furthermore, EA is particularly safe, causes no damage to the myocardium, and can inhibit the systemic inflammatory response in rats with spinal cord injury. This study shows a new perspective on the intervention effect of EA on spinal cord damage and proposes a novel concept for selective therapeutic intervention after SCI.

Acknowledgements

This research was supported by the grants from the National Natural Science Foundation of China (Key Program No. 81891003; General Program No. 81830077; General Program No. 82171379), Shaanxi Provincial Natural Science Foundation Project (No. 2021JQ-925), and General Program of Xi'an Municipal Commission of Health (No. 2021ms05). We thank the Instrument Analysis Center of Xi'an Jiaotong University for fluorescence microscopy imaging and analysis.

Disclosure of conflict of interest

None.

Address correspondence to: Xifang Liu and Dingjun Hao, Xi'an Honghui Hospital, Xi'an Jiaotong University, No. 555, Youyi East Road, Beilin District, Xi'an 710054, China. E-mail: lxfyg2006@126.com (XFL); E-mail: hao_dingjun@163.com (DJH)

References

[1] Wang J, Zhao Y, Tang Y, Li F and Chen X. The role of lncRNA-MEG/miR-21-5p/PDCD4 axis in spinal cord injury. Am J Transl Res 2021; 13: 646-658.

[2] Suzuki H and Sakai T. Current concepts of stem cell therapy for chronic spinal cord injury. Int J Mol Sci 2021; 22: 7435.

[3] Yilmaz T and Kaptanoglu E. Current and future medical therapeutic strategies for the functional repair of spinal cord injury. World J Orthop 2015; 6: 42-55.

[4] Zhao Y, Xiao Z, Chen B and Dai J. The neuronal differentiation microenvironment is essential for spinal cord injury repair. Organogenesis 2017; 13: 63-70.

[5] Ge MH, Tian H, Mao L, Li DY, Lin JQ, Hu HS, Huang SC, Zhang CJ and Mei XF. Zinc attenuates ferroptosis and promotes functional recovery in contusion spinal cord injury by activating Nrf2/GPX4 defense pathway. CNS Neurosci Ther 2021; 27: 1023-1040.

[6] Orr MB, Simkin J, Bailey WM, Kadambi NS, McVicar AL, Veldhorst AK and Gensel JC. Compression decreases anatomical and functional recovery and alters inflammation after contusive spinal cord injury. J Neurotrauma 2017; 34: 2342-2352.

[7] Chen Z, Hong F, Wang Z, Hao D and Yang H. Spermatogonial stem cells are a promising and pluripotent cell source for regenerative medicine. Am J Transl Res 2020; 12: 7048-7059.

[8] Guo Y, Wei W and Chen JD. Effects and mechanisms of acupuncture and electroacupuncture for functional dyspepsia: a systematic review. World J Gastroenterol 2020; 26: 2440-2457.

[9] Malik S, Samaniego T and Guo ZL. Adenosine receptor A2a, but not A1 in the rVLM participates along with opioids in acupuncture-mediated inhibition of excitatory cardiovascular reflexes. Front Neurosci 2019; 13: 1049.

[10] Luo D, Liu L, Liang FX, Yu ZM and Chen R. Electroacupuncture: a feasible Sirt1 promoter which modulates metainflammation in diet-induced obesity rats. Evid Based Complement Alternat Med 2018; 2018: 5302049.

[11] Zhang S, Jin T, Wang L, Liu W, Zhang Y, Zheng Y, Lin Y, Yang M, He X, Lin H, Chen L and Tao J. Electro-acupuncture promotes the differentiation of endogenous neural stem cells via exosomal microRNA 146b after ischemic stroke. Front Cell Neurosci 2020; 14: 223.

[12] Wang Z, Hou Y, Huang Y, Ju F, Liang Z and Li S. Clinical efficacy and safety of electro-acupuncture combined with beraprost sodium and alpha-lipoic acid for diabetic peripheral neuropathy. Am J Transl Res 2022; 14: 612-622.

[13] Chen J, Jian J, Wang J, Shen Z, Shen B, Wang W, Beckel J, de Groat WC, Chermansky C

and Tai C. Low pressure voiding induced by stimulation and 1 kHz post-stimulation block of the pudendal nerves in cats. Exp Neurol 2021; 346: 113860.

[14] Mohan R, Tosolini AP and Morris R. Segmental distribution of the motor neuron columns that supply the rat hindlimb: a muscle/motor neuron tract-tracing analysis targeting the motor end plates. Neuroscience 2015; 307: 98-108.

[15] Zeman RJ, Zhao J, Zhang Y, Zhao W, Wen X, Wu Y, Pan J, Bauman WA and Cardozo C. Differential skeletal muscle gene expression after upper or lower motor neuron transection. Pflugers Arch 2009; 458: 525-535.

[16] Rivlin AS and Tator CH. Effect of duration of acute spinal cord compression in a new acute cord injury model in the rat. Surg Neurol 1978; 10: 38-43.

[17] Hongna Y, Hongzhao T, Quan L, Delin F, Guijun L, Xiaolin L, Fulin G and Zhongren S. Jia-Ji electro-acupuncture improves locomotor function with spinal cord injury by regulation of autophagy flux and inhibition of necroptosis. Front Neurosci 2020; 14: 616864.

[18] Basso DM, Beattie MS, Bresnahan JC, Anderson DK, Faden AI, Gruner JA, Holford TR, Hsu CY, Noble LJ, Nockels R, Perot PL, Salzman SK and Young W. MASCIS evaluation of open field locomotor scores: effects of experience and teamwork on reliability. Multicenter animal spinal cord injury study. J Neurotrauma 1996; 13: 343-359.

[19] Rafique M, Wei T, Sun Q, Midgley AC, Huang Z, Wang T, Shafiq M, Zhi D, Si J, Yan H, Kong D and Wang K. The effect of hypoxia-mimicking responses on improving the regeneration of artificial vascular grafts. Biomaterials 2021; 271: 120746.

[20] Wei P, Chen H, Lin B, Du T, Liu G, He J and You C. Inhibition of the BCL6/miR-31/PKD1 axis attenuates oxidative stress-induced neuronal damage. Exp Neurol 2021; 335: 113528.

[21] Wang K, Gao H, Zhang Y, Yan H, Si J, Mi X, Xia S, Feng X, Liu D, Kong D, Wang T and Ding D. Highly bright AIE nanoparticles by regulating the substituent of Rhodanine for precise early detection of atherosclerosis and drug screening. Adv Mater 2022; 34: e2106994.

[22] Xiong F, Fu C, Zhang Q, Peng L, Liang Z, Chen L, He C and Wei Q. The effect of different acupuncture therapies on neurological recovery in spinal cord injury: a systematic review and network meta-analysis of randomized controlled trials. Evid Based Complement Alternat Med 2019; 2019: 2371084.

[23] Mo YP, Yao HJ, Lv W, Song LY, Song HT, Yuan XC, Mao YQ, Jing QK, Shi SH and Li ZG. Effects of electroacupuncture at governor vessel acupoints on neurotrophin-3 in rats with experimental spinal cord injury. Neural Plast 2016; 2016: 2371875.

[24] Alvarado-Sanchez BG, Salgado-Ceballos H, Torres-Castillo S, Rodriguez-Silverio J, Lopez-Hernandez ME, Quiroz-Gonzalez S, Sanchez-Torres S, Mondragon-Lozano R and Fabela-Sanchez O. Electroacupuncture and curcumin promote oxidative balance and motor function recovery in rats following traumatic spinal cord injury. Neurochem Res 2019; 44: 498-506.

[25] Cheng M, Wu X, Wang F, Tan B and Hu J. Electro-acupuncture inhibits p66shc-mediated oxidative stress to facilitate functional recovery after spinal cord injury. J Mol Neurosci 2020; 70: 2031-2040.

[26] Xu H, Yang Y, Deng QW, Zhang BB, Ruan JW, Jin H, Wang JH, Ren J, Jiang B, Sun JH, Zeng YS and Ding Y. Governor vessel electro-acupuncture promotes the intrinsic growth ability of spinal neurons through activating calcitonin gene-related peptide/alpha-calcium/calmodulin-dependent protein kinase/neurotrophin-3 pathway after spinal cord injury. J Neurotrauma 2021; 38: 734-745.

[27] Zhu XL, Chen X, Wang W, Li X, Huo J, Wang Y, Min YY, Su BX and Pei JM. Electroacupuncture pretreatment attenuates spinal cord ischemia-reperfusion injury via inhibition of high-mobility group box 1 production in a LXA receptor-dependent manner. Brain Res 2017; 1659: 113-120.

[28] Huang S, Tang C, Sun S, Cao W, Qi W, Xu J, Huang J, Lu W, Liu Q, Gong B, Zhang Y and Jiang J. Protective effect of electroacupuncture on neural myelin sheaths is mediated via promotion of oligodendrocyte proliferation and inhibition of oligodendrocyte death after compressed spinal cord injury. Mol Neurobiol 2015; 52: 1870-1881.

[29] Huang SQ, Tang CL, Sun SQ, Yang C, Xu J, Wang KJ, Lu WT, Huang J, Zhuo F, Qiu GP, Wu XY and Qi W. Demyelination initiated by oligodendrocyte apoptosis through enhancing endoplasmic reticulum-mitochondria interactions and Id2 expression after compressed spinal cord injury in rats. CNS Neurosci Ther 2014; 20: 20-31.

[30] Zeng YS, Ding Y, Xu HY, Zeng X, Lai BQ, Li G and Ma YH. Electro-acupuncture and its combination with adult stem cell transplantation for spinal cord injury treatment: a summary of current laboratory findings and a review of literature. CNS Neurosci Ther 2022; 28: 635-647.

[31] Wang YL, Qi YN, Wang W, Dong CK, Yi P, Yang F, Tang XS and Tan MS. Effects of decompression joint Governor Vessel electro-acupuncture on rats with acute upper cervical spinal cord injury. Neural Regen Res 2018; 13: 1241-1246.

[32] Yang Y, Xu HY, Deng QW, Wu GH, Zeng X, Jin H, Wang LJ, Lai BQ, Li G, Ma YH, Jiang B, Ruan JW, Wang YQ, Ding Y and Zeng YS. Electroacupuncture facilitates the integration of a grafted TrkC-modified mesenchymal stem cell-derived neural network into transected spinal cord in rats via increasing neurotrophin-3. CNS Neurosci Ther 2021; 27: 776-791.

[33] Yu J, Wang M, Liu J, Zhang X and Yang S. Effect of electroacupuncture on the expression of agrin and acetylcholine receptor subtypes in rats with tibialis anterior muscular atrophy induced by sciatic nerve injection injury. Acupunct Med 2017; 35: 268-275.

[34] Zhang YT, Jin H, Wang JH, Wen LY, Yang Y, Ruan JW, Zhang SX, Ling EA, Ding Y and Zeng YS. Tail nerve electrical stimulation and electroacupuncture can protect spinal motor neurons and alleviate muscle atrophy after spinal cord transection in rats. Neural Plast 2017; 2017: 7351238.

[35] Zhu L, Jia SJ, Liu TJ, Yan L, Huang DG, Wang ZY, Chen S, Zhang ZP, Zeng W, Zhang Y, Yang H and Hao DJ. Aligned PCL fiber conduits immobilized with nerve growth factor gradients enhance and direct sciatic nerve regeneration. Adv Funct Mater 2020; 30: 2002610.

[36] Yang JH, Lv JG, Wang H and Nie HY. Electroacupuncture promotes the recovery of motor neuron function in the anterior horn of the injured spinal cord. Neural Regen Res 2015; 10: 2033-2039.

[37] Zheng Y, Mao YR, Yuan TF, Xu DS and Cheng LM. Multimodal treatment for spinal cord injury: a sword of neuroregeneration upon neuromodulation. Neural Regen Res 2020; 15: 1437-1450.

[38] Ye GL, Savelieva KV, Vogel P, Baker KB, Mason S, Lanthorn TH and Rajan I. Ligation of mouse L4 and L5 spinal nerves produces robust allodynia without major motor function deficit. Behav Brain Res 2015; 276: 99-110.

[39] Li G, Che MT, Zhang K, Qin LN, Zhang YT, Chen RQ, Rong LM, Liu S, Ding Y, Shen HY, Long SM, Wu JL, Ling EA and Zeng YS. Graft of the NT-3 persistent delivery gelatin sponge scaffold promotes axon regeneration, attenuates inflammation, and induces cell migration in rat and canine with spinal cord injury. Biomaterials 2016; 83: 233-248.

[40] Obradovic AL, Scarpa J, Osuru HP, Weaver JL, Park JY, Pathirathna S, Peterkin A, Lim Y, Jagodic MM, Todorovic SM and Jevtovic-Todorovic V. Silencing the alpha2 subunit of gamma-aminobutyric acid type a receptors in rat dorsal root ganglia reveals its major role in antinociception posttraumatic nerve injury. Anesthesiology 2015; 123: 654-667.

[41] Escobar-Corona C, Torres-Castillo S, Rodriguez-Torres EE, Segura-Alegria B, Jimenez-Estrada I and Quiroz-Gonzalez S. Electroacupuncture improves gait locomotion, H-reflex and ventral root potentials of spinal compression injured rats. Brain Res Bull 2017; 131: 7-17.

[42] Geng X, Zou Y, Li S, Qi R, Jing C, Ding X, Li J and Yu H. Electroacupuncture promotes the recovery of rats with spinal cord injury by suppressing the Notch signaling pathway via the H19/EZH2 axis. Ann Transl Med 2021; 9: 844.

[43] Lee R, Kim IS, Han N, Yun S, Park KI and Yoo KH. Real-time discrimination between proliferation and neuronal and astroglial differentiation of human neural stem cells. Sci Rep 2014; 4: 6319.

[44] Okuda A, Horii-Hayashi N, Sasagawa T, Shimizu T, Shigematsu H, Iwata E, Morimoto Y, Masuda K, Koizumi M, Akahane M, Nishi M and Tanaka Y. Bone marrow stromal cell sheets may promote axonal regeneration and functional recovery with suppression of glial scar formation after spinal cord transection injury in rats. J Neurosurg Spine 2017; 26: 388-395.

[45] Griffin JM, Fackelmeier B, Fong DM, Mouravlev A, Young D and O'Carroll SJ. Astrocyte-selective AAV gene therapy through the endogenous GFAP promoter results in robust transduction in the rat spinal cord following injury. Gene Ther 2019; 26: 198-210.

[46] Wu J, Lu B, Yang R, Chen Y, Chen X and Li Y. EphB2 knockdown decreases the formation of astroglial-fibrotic scars to promote nerve regeneration after spinal cord injury in rats. CNS Neurosci Ther 2021; 27: 714-724.

[47] Pekny M and Pekna M. Astrocyte reactivity and reactive astrogliosis: costs and benefits. Physiol Rev 2014; 94: 1077-1098.

[48] Deng Z, Wei Y, Yao Y, Gao S and Wang X. Let-7f promotes the differentiation of neural stem cells in rats. Am J Transl Res 2020; 12: 5752-5761.